Key comparison BIPM.RI(I)-K3 of the air-kerma standards of the ARPANSA, Australia, and the BIPM in medium-energy x-rays

D T Burns[1], C Kessler[1], M Hanlon[2], T Bailey[2], C Oliver[2], D Butler[2]

[1] Bureau International des Poids et Mesures (BIPM), Pavillon de Breteuil, F-92312 Sèvres
[2] Australian Radiation Protection and Nuclear Safety Agency, Melbourne, Australia

Abstract A key comparison has been made between the air-kerma standards of the ARPANSA and the BIPM in the medium-energy x-ray range. The results show the standards to be in agreement at the level of the expanded uncertainty of the comparison of 8.2 parts in 10^3. The results are analysed and presented in terms of degrees of equivalence, suitable for entry in the BIPM key comparison database.

1. Introduction

An indirect comparison has been made between the air-kerma standards of the Australian Radiation Protection and Nuclear Safety Agency (ARPANSA), Australia, and the Bureau International des Poids et Mesures (BIPM) in the x-ray range from 100 kV to 250 kV. Three cavity ionization chambers were used as transfer instruments. The measurements at the BIPM took place in November 2020 using the reference conditions recommended by the CCRI (CCEMRI 1972). Final data were received from the ARPANSA in August 2021. The comparison was carried out after the implementation of the recommendations of ICRU Report 90 (ICRU 2016) at both laboratories.

2. Determination of the air-kerma rate

For a free-air ionization chamber standard with measuring volume V, the air-kerma rate is determined by the relation

$$\dot{K} = \frac{I}{\rho_{\text{air}} V} \frac{W_{\text{air}}}{e} \frac{1}{1-g_{\text{air}}} \prod_i k_i \qquad (1)$$

where ρ_{air} is the density of air under reference conditions, I is the ionization current under the same conditions, W_{air} is the mean energy expended by an electron of charge e to produce an ion pair in air, g_{air} is the fraction of the initial electron energy lost through radiative processes in air, and $\Pi\, k_i$ is the product of the correction factors to be applied to the standard.

The value used for ρ_{air} at each laboratory is given in Table 1. For use with this dry-air value for ρ_{air}, the ionization current I must be corrected for humidity and for the difference between the density of the air of the measuring volume at the time of measurement and the value given in the table [1]. The value used for W_{air}/e is that recommended in ICRU Report 90 (ICRU 2016), also given in Table 1.

3. Details of the standards

Both free-air chamber standards are of the conventional parallel-plate design. The BIPM air-kerma standard is described in Boutillon (1978) and the changes made to certain correction factors are

[1] For an air temperature $T \sim 293$ K, pressure P and relative humidity ~50 % in the measuring volume, the correction for air density involves a temperature correction T / T_0, a pressure correction P_0 / P and the dry-air humidity correction $k_h = 0.9980$. At the BIPM, the factor 1.0002 is also included to account for the compressibility of dry air between $T \sim 293$ K and $T_0 = 273.15$ K.

given in Burns (2004), Burns and Kessler (2009a) and Burns *et al.* (2009b). The changes made to the standard following the recommendations of ICRU Report 90 are given in Burns and Kessler (2018). The ARPANSA standard and Monte Carlo calculations of correction factors are described in Lye *et al.* (2010). These correction factors were recalculated in 2020 using the egs_fac program (Mainegra-Hing *et al.* 2008). This code evaluates additional correction factors for charged-particle equilibrium, k_{CPE}, and backscatter, k_b. For consistency with the primary standards of the BIPM and national metrology institutes (NMIs), k_b has not been included in the present comparison. However, the authors recognize that the photon fluence seen by a cavity chamber under calibration includes a component due to scatter in the air between the x-ray source and the chamber that is not seen by a free-air chamber, which is essentially a 'narrow beam' measurement. Although this scatter component will largely cancel for a cavity chamber used as a transfer instrument during a comparison of free-air chambers, a correction for this effect is required, at least in principle, for the calibration of a cavity chamber. A consistent evaluation and implementation of such a correction factor, if found to be significant, will be considered for the future.

The new set of correction factors includes the recommendations of ICRU Report 90. The ARPANSA standard was previously compared with the BIPM standard in an indirect comparison carried out in 2010, the results of which are reported in Burns *et al.* (2012). The main dimensions, the measuring volume and the polarizing voltage for each standard are shown in Table 2.

Table 1. Physical constants used in the determination of the air-kerma rate

Constant	Value	u_i [a]
ρ_{air} [b] (BIPM)	1.2930 kg m^{-3}	0.0001
ρ_{air} [c] (ARPANSA)	1.2047 kg m^{-3}	0.0001
W_{air} / e	33.97 J C^{-1}	0.0035

[a] u_i is the relative standard uncertainty.
[b] Density of dry air at T_0 = 273.15 K and P_0 = 101.325 kPa.
[c] Density of dry air at T_0 = 293.15 K and P_0 = 101.325 kPa.

Table 2. Main characteristics of the standards

Standard	BIPM M-01	ARPANSA
Aperture diameter / mm	9.939	8.0476
Air path length / mm	281.5	297
Collecting length / mm	60.004	100.849
Electrode separation / mm	180	200
Collector width / mm	200	300
Measuring volume / mm^3	4655.4	5129.7
Polarizing voltage / V	4000	5000

4. The transfer instruments

4.1 Determination of the calibration coefficient for a transfer instrument

The air-kerma calibration coefficient N_K for a transfer instrument is given by the relation

$$N_K = \frac{\dot{K}}{I_{\mathrm{tr}}} \tag{2}$$

where $\dot{K}$ is the air-kerma rate determined by the standard using Equation (1) and I_{tr} is the ionization current measured by the transfer instrument and the associated current-measuring system. The current I_{tr} is corrected to the standard conditions of air temperature, pressure and relative humidity chosen for the comparison (T = 293.15 K, P = 101.325 kPa, RH = 50 %). No humidity correction has been applied to the current measured using the transfer instruments, on the basis that the BIPM laboratory is maintained with a relative humidity in the range from 40 % to 55 % and the ARPANSA laboratory in the range from 30 % to 75 %.

To derive a comparison result from the calibration coefficients $N_{K,\mathrm{BIPM}}$ and $N_{K,\mathrm{NMI}}$ measured, respectively, at the BIPM and at an NMI, differences in the radiation qualities must be taken into account. Normally, each quality used for the comparison has the same nominal generating potential at each institute, but the half-value layers (HVLs) may differ. A radiation quality correction factor k_Q is derived for each comparison quality Q. This corrects the calibration coefficient $N_{K,\mathrm{NMI}}$ determined at the NMI into one that applies at the 'equivalent' BIPM quality and is derived by interpolation of the $N_{K,\mathrm{NMI}}$ values in terms of log(HVL). The comparison result at each quality is then taken as

$$R_{K,\mathrm{NMI}} = \frac{k_{\mathrm{Q}} N_{K,\mathrm{NMI}}}{N_{K,\mathrm{BIPM}}} \tag{3}$$

In practice, the half-value layers normally differ by only a small amount and k_Q is close to unity.

4.2 Details of the transfer instruments

Three thimble-type cavity ionization chambers belonging to the ARPANSA, an NE 2571, an IBA FC65G and a PTW 30013, were used as transfer instruments for the comparison. The same NE 2571 chamber was also used during the 2010 comparison. The main characteristics of the chambers are given in Table 3. Each chamber, without build-up cap, was positioned with the stem perpendicular to the beam direction and with the line on the stem facing the source. The reference point for each chamber is located 13 mm from the thimble tip.

5. Calibration at the BIPM

5.1 The BIPM irradiation facility and reference radiation qualities

The BIPM medium-energy x-ray laboratory houses a high-stability generator and a tungsten-anode x-ray tube with a 3 mm beryllium window. In addition to the aluminium filter of thickness 1.203 mm used for the 100 kV radiation quality, an aluminium filter of thickness 2.228 mm is added for all radiation qualities to compensate for the decrease in filtration that occurred when the original BIPM x-ray tube (with an aluminium window of approximately 3 mm) was replaced in June 2004. Two voltage dividers monitor the tube voltage and a voltage-to-frequency converter combined with data transfer by optical fibre measures the anode current. No transmission monitor is used. For a given radiation quality, the standard deviation of repeat air-kerma rate determinations over many months is typically 3 parts in 10^4. The radiation qualities used in the range from 100 kV to 250 kV are those recommended by the CCRI (CCEMRI 1972) and are given in Table 4.

The irradiation area is temperature controlled at around 20 °C and is stable over the duration of a calibration to typically 0.2 °C. Two calibrated thermistors measure the temperature of the ambient air and the air inside the BIPM standard (which is controlled at 25 °C). Air pressure is measured by means of a calibrated barometer.

Table 3. Main characteristics of the transfer chambers

Chamber type	NE 2571	IBA FC65G	PTW 30013
Serial number	3075	1612	7470
Geometry	thimble	thimble	thimble
External diameter / mm	7.0	7.0	6.9
Wall material	graphite	graphite	0.09 mm graphite 0.33 mm PMMA
Wall thickness / mm	0.36	0.4	0.42
Nominal volume / cm^3	0.7	0.65	0.6
Polarizing potential / V	+250 [a]	+300 [a]	–400 [a]

[a] At the ARPANSA, the stated potential is applied to the central collector, the outer wall remaining at virtual ground potential. At the BIPM, a potential of opposite sign to that stated was applied to the outer wall of the chamber, the collector remaining at virtual ground.

Table 4. Characteristics of the BIPM reference radiation qualities

Radiation quality	100 kV	135 kV	180 kV	250 kV
Generating potential / kV	100	135	180	250
Inherent Be filtration / mm	3	3	3	3
Additional Al filtration / mm	3.431	2.228	2.228	2.228
Additional Cu filtration / mm	-	0.232	0.485	1.570
Al HVL / mm	4.030	-	-	-
Cu HVL / mm	0.149	0.489	0.977	2.484
$(\mu/\rho)_{air}$ [a] / $cm^2\ g^{-1}$	0.290	0.190	0.162	0.137
$\dot{K}_{BIPM}$ / mGy s^{-1}	0.50	0.50	0.50	0.50

[a] Measured at the BIPM using an evacuated tube of length 280 mm.

5.2 The BIPM standard and correction factors

The reference plane for the BIPM standard was positioned at 1200 mm from the radiation source, with a reproducibility of 0.03 mm. The standard was aligned laterally on the beam axis to an

estimated uncertainty of 0.1 mm. The beam diameter in the reference plane is 98 mm for all radiation qualities.

During the calibration of the transfer chambers, measurements using the BIPM standard were made using positive polarity only. A correction factor of 1.00015 was applied to correct for the known polarity effect in the standard. The leakage current for the BIPM standard, relative to the ionization current, was measured to be around 1 part in 10^4.

The correction factors applied to the ionization current measured at each radiation quality using the BIPM standard, together with their associated uncertainties, are given in Table 5. The factor k_a corrects for the attenuation of the x-ray fluence along the air path between the reference plane and the centre of the collecting volume. It is evaluated using the measured mass attenuation coefficients for air $(\mu/\rho)_{air}$ given in Table 4. In practice, the values used for k_a take account of the temperature and pressure of the air in the standard. Ionization current measurements (both for the standard and for transfer chambers) are also corrected for changes in air attenuation arising from variations in the temperature and pressure of the ambient air between the radiation source and the reference plane.

Table 5. Correction factors for the BIPM standard

Radiation quality	100 kV	135 kV	180 kV	250 kV	u_{iA}	u_{iB}
Air attenuation k_a [a]	1.0099	1.0065	1.0055	1.0047	0.0002	0.0001
Photon scatter k_{sc}	0.9952	0.9959	0.9964	0.9974	-	0.0003
Fluorescence k_{fl}	0.9985	0.9992	0.9994	0.9999	-	0.0003
Electron loss k_e	1.0000	1.0015	1.0047	1.0085	-	0.0005
Initial ionization k_{ii}	0.9980	0.9980	0.9981	0.9986	-	0.0005
Energy dependence of W_{air} k_W						
Ion recombination k_s	1.0010	1.0010	1.0010	1.0010	0.0002	0.0001
Polarity k_{pol}	1.0002	1.0002	1.0002	1.0002	0.0001	-
Field distortion k_d	1.0000	1.0000	1.0000	1.0000	-	0.0007
Diaphragm correction k_{dia}	0.9995	0.9993	0.9991	0.9980	-	0.0003
Wall transmission k_p	1.0000	1.0000	0.9999	0.9988	0.0001	-
Humidity k_h	0.9980	0.9980	0.9980	0.9980	-	0.0003
$1 - g_{air}$	0.9999	0.9999	0.9998	0.9997	-	0.0001

[a] Values for the BIPM reference conditions of 293.15 K and 101.325 kPa; each measurement is corrected using the air temperature and pressure measured at the time.

Two new correction factors, k_{ii} and k_W, are implemented following the recommendations of ICRU Report 90 (ICRU 2016) and presented as the product $k_{ii}k_W$ by Burns and Kessler (2018). Both correction factors are related to the mean energy expended in dry air per ion pair formed, W_{air}. The initial ionization correction factor k_{ii} accounts for the fact that the definition of W_{air} does not include the charge of the initial charged particle, while the correction factor k_W accounts for the rapid increase in the value of W_{air} at electron energies below around 10 keV.

5.3 Transfer chamber positioning and calibration at the BIPM

The reference point for each transfer chamber was positioned in the reference plane (1200 mm from the radiation source), with a reproducibility of 0.03 mm. Each chamber was aligned on the beam axis to an estimated uncertainty of 0.1 mm.

The leakage current was measured before and after each series of ionization current measurements and a correction made using the mean value. The relative leakage current was typically 1 part in 10^4 for each of the three chambers.

The calibration procedure involves measurements with a transfer chamber and with the standard at a given radiation quality before proceeding to the next quality, with a period of typically 10 minutes following a change of quality to allow the generator and tube to stabilize. For each transfer chamber and at each radiation quality, two or more sets of seven measurements were made, each measurement with integration time between 60 s and 100 s. The relative standard uncertainty of the mean ionization current for each set was typically 1 part in 10^4. Based on the results of repeat calibrations including chamber repositioning, an uncertainty component of 3 parts in 10^4 is included in Table 11 for the short-term reproducibility of the calibration coefficients determined at the BIPM.

6. Calibration at the ARPANSA

6.1 The ARPANSA irradiation facility and reference radiation qualities

The medium-energy x-ray facility at the ARPANSA, replaced in 2016, comprises two 160 kV high-frequency generators (Gulmay) and a tungsten-anode x-ray tube (Comet) with a 3 mm beryllium window. The generator voltage has been verified indirectly using a spectroscopic method to estimate the highest energy x-ray in the spectrum, the results in agreement with the expected values to better than 3 parts in 10^2; the HVLs are measured annually to monitor any changes. The x-ray output is monitored by means of a large-area transmission ionization chamber (PTW 34014 with active diameter 14.8 cm and volume 86 cm^3), the chamber windows introducing an additional filtration (10.65 mg cm^{-2}) of polyimide and graphite. The monitor chamber along with the apertures and filters were also replaced in 2016 as a part of a commercial irradiator system (Hopewell Designs). The characteristics of the ARPANSA realization of the CCRI comparison qualities (CCEMRI 1972) are given in Table 6.

The primary standard and calibration method remain the same as for the comparison in 2010, although the electrometers were replaced by the PTW UNIDOS Webline Type 10022 and minor changes were made to the electrical connections and cables. The irradiation area is temperature controlled at around 22 °C and is stable to better than 0.5 °C over a typical set of measurements. The monitor chamber temperature, the ambient air temperature and the temperature inside the primary standard are measured using calibrated thermistors. A calibrated barometer measures the atmospheric pressure in the laboratory and a hygrometer measures the humidity inside the primary standard.

The short-term reproducibility of the ratio of the standard chamber to the monitor chamber is typically better than 5 parts in 10^4. However when the measurement sequence is repeated after several hours the reproducibility is less good; the standard deviation of a series of measurements over several days may be as high as 3 parts in 10^3. Following investigation, it is believed that the variations are the result of temperature changes in the room which are not fully accounted for by the temperature corrections, although isolating the exact cause has proved difficult. It is not currently possible to remove all sources of temperature variation because the room is not sealed and the high-voltage generator is air cooled, which presents a heat source inside the room. These

issues are covered by an uncertainty contribution for the reproducibility of transfer chamber calibrations (Table 11) of 3 parts in 10^3.

Table 6. Characteristics of the ARPANSA reference radiation qualities

Radiation quality	100 kV	135 kV	180 kV	250 kV
Generating potential / kV	100	135	180	250
Inherent Be filtration / mm	3	3	3	3
Additional Al filtration / mm	3.433	2.214	2.273	2.230
Additional Cu filtration / mm	-	0.230	0.485	1.570
Al HVL / mm	4.085	-	-	-
Cu HVL / mm	0.152	0.480	0.958	2.447
$(\mu/\rho)_{air}$ [a] / cm^2 g^{-1}	0.296	0.200	0.172	0.145
$\dot{K}_{ARPANSA}$ / mGy s^{-1}	1.9	1.8	2.0	2.0

[a] The ARPANSA mass attenuation coefficients for air are calculated.

6.2 The ARPANSA standard and correction factors

The reference plane for the ARPANSA standard (the inner surface of the diaphragm) was positioned at 1000 mm from the radiation source, with a reproducibility of 0.5 mm. The standard was aligned laterally on the beam axis to an estimated uncertainty of 0.5 mm. The beam diameter in the reference plane is 110 mm for all radiation qualities.

During the calibration of the transfer chambers, measurements using the ARPANSA standard were made using negative polarity only. A correction factor of unity with a standard uncertainty of 1 part in 10^4 is applied to take into account any small polarity effect in the standard. The leakage current was measured before and after each radiation measurement. In the majority of cases it was less than 0.2 pA, which represents some 6 parts in 10^4 for the CCRI beams.

The correction factors applied to the ionization current measured at each radiation quality using the ARPANSA standard, together with their associated uncertainties, are given in Table 7. The correction factor k_a is evaluated using the calculated mass attenuation coefficients given in Table 6 for the reference air density given in Table 1. Variations in k_a due to the temperature and pressure of the air in the standard at the time of the measurements are not taken into account. These effects are included in the uncertainty stated for k_a in Table 7. The correction for scattered radiation, k_{sc}, now includes the correction for fluorescence previously treated separately as the factor k_{fl}. As for the BIPM standard, two new correction factors, k_{ii} and k_W, are implemented as the product $k_{ii}k_W$.

6.3 Transfer chamber positioning and calibration at the ARPANSA

The reference point for each transfer chamber was positioned at the reference distance with a reproducibility of 1 mm or better, resulting in a variation in response when each chamber was positioned. The resulting uncertainty is included in the estimate for reproducibility (see Section 9). Lateral alignment on the beam axis was estimated to be within 2 mm.

The measurement sequence starts with a leakage current measurement and then the transfer chamber current is measured for each radiation quality with only a short interruption while the

filter, generating voltage and tube current are changed under computer control. The sequence ends with a second leakage measurement. For each quality, the ionization current was measured for typically 300 s by taking a series of 300 readings at a rate of 1 reading per second. The relative standard uncertainty of the mean for each quality was typically less than 2 parts in 10^4 for each transfer chamber. A correction was made using the leakage current measured at the start of the sequence, the relative leakage being typically 1 part in 10^4 for each of the three chambers.

The entire sequence is repeated for the primary standard to give one set of calibrations of the transfer chamber. Each chamber was calibrated in this way at least four times before and four times after the chambers were measured at the BIPM.

Table 7. Correction factors for the ARPANSA standard

Radiation quality	100 kV	135 kV	180 kV	250 kV	$u_{i\mathrm{A}}$	$u_{i\mathrm{B}}$
Air attenuation k_a	1.0107	1.0072	1.0062	1.0052	-	0.0011
Photon scatter k_{sc} (incl. fluorescence)	0.9928	0.9941	0.9950	0.9962	-	0.0007
Electron loss k_e	1.0001	1.0005	1.0021	1.0047	-	0.0005
Initial ionization k_{ii}	0.9979	0.9980	0.9982	0.9987	-	0.0004
Energy dependence of W_{air} k_W						
Ion recombination k_s[a]	1.0000	1.0000	1.0000	1.0000	-	0.0005
Polarity k_{pol}	1.0000	1.0000	1.0000	1.0000	-	0.0001
Field distortion k_d	1.0000	1.0000	1.0000	1.0000	-	0.0005
Diaphragm correction k_{tr}[b]	0.9993	0.9985	0.9978	0.9951	-	0.0005
Wall transmission k_p	1.0000	1.0000	1.0000	1.0000	-	0.0003
Humidity k_h[c]	0.9977	0.9977	0.9977	0.9977	-	0.0003
$1 - g_{air}$	1.0000	1.0000	1.0000	1.0000	-	0.0003
Charged-particle equilibrium k_{CPE}	0.9999	0.9999	0.9999	0.9998	-	0.0001

[a] Historical measurements indicate a value of 1.0005, but this correction is not applied at the ARPANSA.
[b] Includes photon transmission and scattering in the diaphragm.
[c] Calculated from the relative humidity *RH* as k_h = 0.995767 + 4.5E-5**RH*, where 30 % < *RH* < 75 %, using the data given in ICRU Report 90 (ICRU 2016).

7. Additional considerations for transfer chamber calibrations

7.1 Ion recombination, polarity, radial non-uniformity and field size

As can be seen from Tables 4 and 6, the air-kerma rates at the ARPANSA are almost a factor of four greater than those at the BIPM. However, for these thimble-type chambers the difference in volume recombination at the two laboratories is well below 1 part in 10^4. Consequently, no corrections are applied for ion recombination. Each transfer chamber was used with the same polarity at each laboratory and so no corrections are applied for polarity effects in the transfer chambers.

No correction is applied at either laboratory for the radial non-uniformity of the radiation field. For small chambers with cavity dimensions below 2 cm, the effect should be small and will cancel to some extent at the two laboratories. A relative standard uncertainty of 3 parts in 10^4 is introduced in Table 12 for this effect. Additionally, in the ARPANSA arrangement the heel effect is vertical and parallel with the long axis of the thimble cavity (at the BIPM they are perpendicular) so that, when combined with the uncertainty in the vertical positioning of the transfer chamber, a larger uncertainty arises which the ARPANSA estimate to be 1 part in 10^3, included in Table 11.

The radiation field size at the ARPANSA, 110 mm in diameter, is only marginally greater than the BIPM beam diameter of 98 mm. The effect of this on the transfer chamber calibrations is assumed to be negligible.

7.2 Radiation quality correction factors k_Q

As noted in Section 4.1, slight differences in radiation qualities might require a correction factor k_Q. From Tables 4 and 6 it is evident that the radiation qualities at the BIPM and at the ARPANSA are reasonably matched in terms of HVL. A set of correction factors k_Q was evaluated for each transfer chamber from a fit to the results obtained at the BIPM; the results are included in Table 8 and are applied according to Equation (3). A standard uncertainty for these factors of 2 parts in 10^4 is included in Table 12.

8. Comparison results

The calibration coefficients $N_{K,\mathrm{ARPANSA}}$ and $N_{K,\mathrm{BIPM}}$ for the transfer chambers are given in Table 8 and the comparison results $R_{K,\mathrm{ARPANSA}}$ evaluated according to Equation (3) are presented in Table 9. For each quality, the final result in bold in Table 9 is evaluated as the unweighted mean for the three transfer chambers. The standard uncertainty u_{tr} arising from the variation in the results for the three chambers is also given for each radiation quality. However, these values are smaller than the changes observed in the pre- and post-comparison $N_{K,\mathrm{ARPANSA}}$ values, as discussed in Section 9. Also given in Table 9 are the results of the previous comparison of the ARPANSA and BIPM standards (Burns *et al.* 2012), revised for the changes made to both standards.

9. Uncertainties

The uncertainties associated with the primary standards are listed in Table 10 and those for the transfer chamber calibrations in Table 11. The combined standard uncertainty u_c for the comparison results $R_{K,\mathrm{ARPANSA}}$ is presented in Table 12. This takes into account correlation in the type B uncertainties associated with the physical constants, the humidity correction and the product of the correction factors $k_{\mathrm{ii}}k_W$. Correlation in the values for k_{sc}, k_{fl} and k_{e} at the BIPM and at the ARPANSA, derived from Monte Carlo calculations in each laboratory, are taken into account in an approximate way by assuming half of the uncertainty value for each factor at each laboratory. This is consistent with the analysis of the results of the BIPM comparisons in medium-energy x-rays in terms of degrees of equivalence described in Burns (2003).

A significant source of uncertainty arises from the reproducibility of the transfer chamber calibrations at the ARPANSA. This was evaluated from the standard deviation of eight or more repeat measurements on different days, before and after the chambers were measured at the BIPM. While the ARPANSA has long been aware of a significant day-to-day variation in calibration results (a standard deviation of 3 parts in 10^3 is typical), it was assumed until now that these variations were random and that this uncertainty could therefore be reduced by repeat measurement. However, for the present comparison a systematic difference was observed between the pre- and post- comparison measurements at the BIPM of up to 3 parts in 10^3 across all three transfer chambers. Based on their long-term behaviour and the fact that all three chambers exhibited a similar shift, it is unlikely that the chambers themselves have changed significantly. Instead, it is postulated that the observed changes are the result of systematic differences in the

laboratory temperature profile during the pre- and post-comparison measurements. Other possible causes, such as a change in the generator kV, should have also produced a change in HVL, which was not observed. An uncertainty component of 3 parts in 10^3 has been included in Table 11 for the reproducibility at the ARPANSA. This estimate includes a contribution from the uncertainty in transfer chamber positioning.

Table 8. Calibration coefficients for the transfer chambers

Radiation quality	100 kV	135 kV	180 kV	250 kV
Transfer chamber NE 2571-3075				
$N_{K,\mathrm{ARPANSA}}$ (pre-comp) / Gy μC^{-1}	41.99	41.68	41.34	41.01
$N_{K,\mathrm{ARPANSA}}$ (post-comp) / Gy μC^{-1}	41.93	41.57	41.23	40.86
$N_{K,\mathrm{BIPM}}$ / Gy μC^{-1}	41.79	41.38	41.05	40.75
k_Q	1.0002	0.9997	0.9998	0.9998
Transfer chamber IBA FC65G-1612				
$N_{K,\mathrm{ARPANSA}}$ (pre-comp) / Gy μC^{-1}	44.90	44.55	44.05	43.54
$N_{K,\mathrm{ARPANSA}}$ (post-comp) / Gy μC^{-1}	44.87	44.45	43.94	43.38
$N_{K,\mathrm{BIPM}}$ / Gy μC^{-1}	44.71	44.23	43.73	43.21
k_Q	1.0002	0.9996	0.9997	0.9998
Transfer chamber PTW 30013-7470				
$N_{K,\mathrm{ARPANSA}}$ (pre-comp) / Gy μC^{-1}	48.04	48.09	48.10	48.12
$N_{K,\mathrm{ARPANSA}}$ (post-comp) / Gy μC^{-1}	48.02	47.95	47.93	47.93
$N_{K,\mathrm{BIPM}}$ / Gy μC^{-1}	47.89	47.81	47.78	47.85
k_Q	1.0000	1.0000	1.0000	1.0000

Table 9. Comparison results

Radiation quality	100 kV	135 kV	180 kV	250 kV
$R_{K,\mathrm{ARPANSA}}$ using NE 2571-3075	1.0042	1.0056	1.0055	1.0044
$R_{K,\mathrm{ARPANSA}}$ using IBA FC65G-1612	1.0041	1.0057	1.0058	1.0055
$R_{K,\mathrm{ARPANSA}}$ using PTW 30013-7470	1.0030	1.0044	1.0049	1.0037
Standard uncertainty u_{tr}	0.0004	0.0004	0.0003	0.0005
Final $R_{K,\mathrm{ARPANSA}}$	**1.0038**	**1.0052**	**1.0054**	**1.0045**
Revised results of 2010 comparison	*1.0033*	*1.0048*	*1.0050*	*1.0041*

10. Discussion

The comparison results presented in Table 9 show the ARPANSA and the BIPM standards to be in agreement at the level of the expanded uncertainty of the comparison of 8.2 parts in 10^3. The results for the four qualities are consistent at the level of 1 part in 10^3.

It is also of note that the results are in very good agreement for all four qualities with those obtained during the comparison in 2010 (corrected for changes to both standards in the interim period), as given in the final row of Table 9. This result is perhaps surprising given the stated ARPANSA uncertainty of 3 parts in 10^3 for the reproducibility of their calibration coefficients (Table 11).

Table 10. Uncertainties associated with the standards

Standard	BIPM		ARPANSA	
Relative standard uncertainty	$u_{i\mathrm{A}}$	$u_{i\mathrm{B}}$	$u_{i\mathrm{A}}$	$u_{i\mathrm{B}}$
Ionization current	0.0002	0.0002	0.0005	0.0009
Positioning	0.0001	0.0001	-	0.0010
Volume	0.0001	0.0005	-	0.0008
Correction factors (excl. k_h)	0.0003	0.0011	-	0.0017
Humidity k_h	-	0.0003	-	0.0003
Physical constants	-	0.0035	-	0.0035
$\dot{K}$	0.0004	0.0037	0.0005	0.0042

Table 11. Uncertainties associated with the calibration of the transfer chambers

Laboratory	BIPM		ARPANSA	
Relative standard uncertainty	$u_{i\mathrm{A}}$	$u_{i\mathrm{B}}$	$u_{i\mathrm{A}}$	$u_{i\mathrm{B}}$
$\dot{K}$	0.0004	0.0037	0.0005	0.0042
I_tr	0.0002	0.0002	0.0005	0.0005
Positioning of transfer chamber	0.0001	-	- [a]	-
Reproducibility	0.0003	-	0.0030	-
Beam non-uniformity	-	-	-	0.0010 [b]
$N_{K,\mathrm{lab}}$	0.0005	0.0037	0.0031	0.0043

[a] Uncertainties related to transfer chamber positioning are included in the ARPANSA estimate for reproducibility, see Section 9.
[b] Beam non-uniformity in relation to the heel effect at the ARPANSA is discussed in Section 7.

Table 12. Uncertainties associated with the comparison results

Relative standard uncertainty	u_{iA}	u_{iB}
$N_{K,ARPANSA}$ / $N_{K,BIPM}$	0.0031	0.0027 [a]
Beam non-uniformity	-	0.0003
k_Q	-	0.0002
$R_{K,ARPANSA}$	0.0031	0.0027
	u_c = 0.0041	

[a] Takes account of correlation in type B uncertainties.

11. Degrees of Equivalence

The analysis of the results of BIPM comparisons in medium-energy x-rays in terms of degrees of equivalence is described in Burns (2003). Following a decision of the CCRI, the BIPM determination of the air-kerma rate is taken as the key comparison reference value, for each of the CCRI radiation qualities. It follows that for each laboratory *i* having a BIPM comparison result x_i with combined standard uncertainty u_i, the degree of equivalence with respect to the reference value is the relative difference $D_i = (K_i - K_{BIPM,i}) / K_{BIPM,i} = x_i - 1$ and its expanded uncertainty $U_i = 2\,u_i$. The results for D_i and U_i, expressed in mGy/Gy and including those of the present comparison, are shown in Table 13 and in Figure 1.

When required, the degree of equivalence between two laboratories *i* and *j* can be evaluated as the difference $D_{ij} = D_i - D_j$ and its expanded uncertainty $U_{ij} = 2u_{ij}$, both expressed in mGy/Gy. In evaluating u_{ij}, account should be taken of correlation between u_i and u_j (Burns 2003).

12. Conclusions

The key comparison BIPM.RI(I)-K3 for the determination of air kerma in medium-energy x-rays shows the standards of the ARPANSA and the BIPM to be in agreement at the level of the expanded uncertainty of the comparison of 8.2 parts in 10^3.

Tables and graphs of degrees of equivalence, including those for the ARPANSA, are presented for entry in the BIPM key comparison database. Note that the data presented in the tables, while correct at the time of publication of the present report, become out of date as laboratories make new comparisons with the BIPM. The formal results under the CIPM MRA are those available in the BIPM key comparison database (KCDB 2021).

Table 13. Degrees of equivalence

For each laboratory *i*, the degree of equivalence with respect to the key comparison reference value is the difference D_i and its expanded uncertainty U_i. Laboratory names in red indicate participation in BIPM.RI(I)-K3, blue in APMP.RI(I)-K3 and green in SIM.RI(I)-K3.

	100 kV		135 kV		180 kV		250 kV	
Lab *i*	D_i /(mGy/Gy)	U_i /(mGy/Gy)	D_i /(mGy/Gy)	U_i /(mGy/Gy)	D_i /(mGy/Gy)	U_i /(mGy/Gy)	D_i /(mGy/Gy)	U_i /(mGy/Gy)
MKEH	**-0.4**	7.0	**0.9**	7.0	**0.4**	7.0	**0.4**	7.0
PTB	**2.7**	5.2	**4.5**	5.2	**4.9**	5.2	**5.5**	5.2
ENEA	**3.9**	6.2	**4.2**	6.2	**7.3**	6.2	**5.6**	6.2
BEV	**3.2**	6.4	**4.7**	6.4	**4.1**	6.4	**1.1**	6.4
NRC	**3.1**	6.6	**2.3**	6.6	**1.3**	6.6	**0.4**	6.6
NMIJ	**-0.8**	6.2	**-1.4**	6.2	**-2.4**	6.2	**-3.7**	6.2
VSL	**-1.0**	6.4	**-0.4**	6.4	**0.0**	6.4	**-2.1**	6.4
NIST	**-2.2**	7.8	**-3.3**	7.8	**-2.7**	7.8	**-5.8**	7.8
NIM	**7.2**	6.2	**5.4**	6.2	**6.1**	6.2	**6.0**	6.2
NPL	**0.4**	6.8	**0.0**	6.8	**-2.5**	6.8	**-4.4**	6.8
LNE-LNHB	**0.5**	7.6	**-0.5**	7.6	**-1.0**	7.6	**-2.8**	7.6
VNIIM	**0.5**	3.8	**1.0**	3.8	**1.7**	3.8	**2.2**	3.8
GUM	**6.9**	6.0	**3.2**	6.0	**3.6**	6.0	**2.7**	6.0
ARPANSA	**3.8**	8.2	**5.2**	8.2	**5.4**	8.2	**4.5**	8.2
INER	**3.7**	4.6	**4.3**	4.6	**6.0**	4.6	**5.5**	4.6
Nuc. Malaysia	**14.2**	12.0	**16.2**	12.0	**15.0**	12.0	**15.9**	12.0
DMSc	**-3.1**	11.8	**4.2**	11.8	**9.6**	11.8	**13.0**	11.8
BARC	**8.5**	13.8					**14.8**	13.8
NMISA	**4.5**	5.6	**2.0**	5.6	**4.8**	5.6	**7.5**	5.6
KRISS	**-8.4**	5.2	**1.1**	5.2	**6.6**	5.2	**7.6**	5.2
IAEA	**4.3**	7.4	**9.2**	7.4	**13.1**	7.4	**14.0**	7.4
CNEA	**-6.0**	14.3	**1.1**	14.3	**2.1**	14.3	**1.4**	14.3
LMNRI/IRD	**-9.5**	12.1	**-9.4**	12.1	**-8.0**	12.1	**-8.5**	12.1
ININ	**-9.3**	16.1	**-12.1**	16.1	**-11.1**	16.1	**-12.0**	16.1

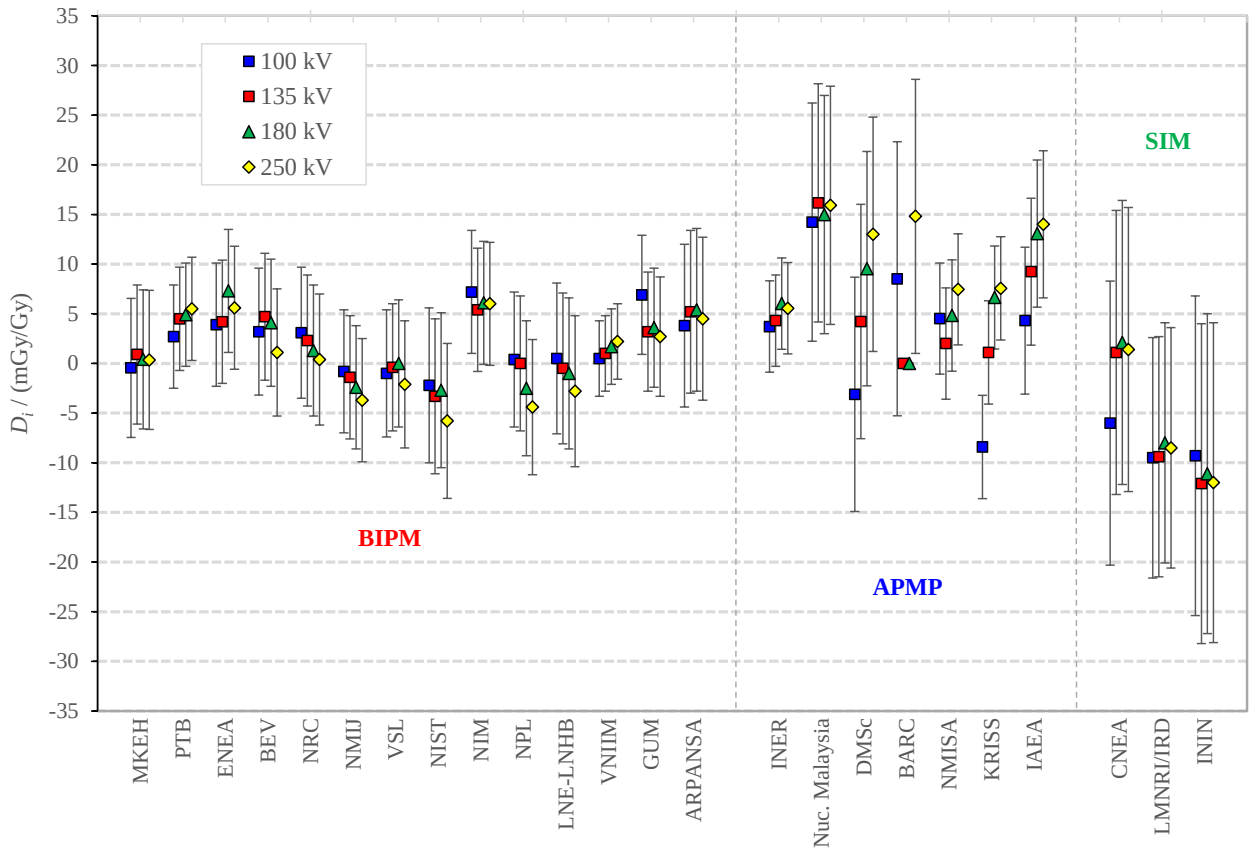

Figure 1. Degrees of equivalence for each laboratory *i* with respect to the key comparison reference value. Results to the left are for the ongoing international comparison BIPM.RI(I)-K3, those in the middle section are for the regional comparison APMP.RI(I)-K3 and those to the right are for the regional comparison SIM.RI(I)-K3.

References

Boutillon M 1978 Mesure de l'exposition au BIPM dans le domaine des rayons X de 100 à 250 kV *Rapport BIPM*-78/3

Burns D T 2003 Degrees of equivalence for the key comparison BIPM.RI(I)-K3 between national primary standards for medium-energy x-rays *Metrologia* **40** *Tech. Suppl.* 06036

Burns D T 2004 Changes to the BIPM primary air-kerma standards for x-rays *Metrologia* **41**, L3

Burns D T, Kessler C 2009a Diaphragm correction factors for free-air chamber standards for air kerma in x-rays *Phys. Med. Biol.* **54** 2737–45

Burns D T, Kessler C 2018 Re-evaluation of the BIPM international dosimetry standards on adoption of the recommendations of ICRU Report 90 *Metrologia* **55** R21

Burns D T, Kessler C, Allisy P J 2009b Re-evaluation of the BIPM international standards for air kerma in x-rays *Metrologia* **46** L21–23

Burns D T, Lye J E, Roger P, Butler D J 2012 Key comparison BIPM.RI(I)-K3 of the air-kerma standards of the ARPANSA, Australia and the BIPM in medium-energy x-rays *Metrologia* **49** *Tech. Suppl.* 06007

CCEMRI 1972 Qualités de rayonnement Comité Consultatif pour les Étalons de Mesures des Rayonnements Ionisants (Section I) 2nd *meeting* R15–1

ICRU 2016 Key data for ionizing-radiation dosimetry: Measurement standards and applications J. ICRU **14** Report 90 (Oxford University Press)

KCDB 2021 The BIPM key comparison database is available online at http://kcdb.bipm.org/

Lye J E, Butler D J, Webb D V 2010 Monte Carlo correction factors for the ARPANSA kilovoltage free-air chambers and the effect of moving the limiting aperture *Metrologia* **47** 11–20

Mainegra-Hing E, Reynaert N, Kawrakow I 2008 Novel approach for the Monte Carlo calculation of free-air chamber correction factors *Med. Phys.* **35** 3650–60